Silibinin preferentially radiosensitizes prostate cancer by inhibiting DNA repair signaling

Dhanya K. Nambiar[1,2], **Paulraj Rajamani**[2], **Gagan Deep**[4], **Anil K. Jain**[4], **Rajesh Agarwal**[4], and **Rana P. Singh**[1,3,*]

[1]Cancer Biology Laboratory, School of Life Sciences, Jawaharlal Nehru University, New Delhi, India

[2]School of Environmental Sciences, Jawaharlal Nehru University, New Delhi, India

[3]School of Life Sciences, Central University of Gujarat, Gandhinagar, India

[4]Department of Pharmaceutical Sciences, Skaggs School of Pharmacy and Pharmaceutical Sciences, University of Colorado Denver, Aurora, Colorado, USA

Abstract

Radiotherapy, a frequent mode of cancer treatment, is often restricted by dose-related toxicity and development of therapeutic resistance. To develop a novel and selective radiosensitizer, we studied the radiosensitizing effects and associated mechanisms of silibinin in prostate cancer (PCa). The radiosensitizing effect of silibinin with ionizing radiation (IR) was assessed on radioresistant PCa cell lines by clonogenic, cell cycle, cell death and DNA repair assays. Tumor xenograft growth, immunohistochemical (IHC) analysis of tumor tissues, and toxicity-related parameters were measured *in vivo*. Silibinin (25 μM) enhanced IR (2.5-10 Gy)-caused inhibition (up to 96%, P<0.001) of colony formation selectively in PCa cells, and prolonged and enhanced IR-caused G2/M arrest, apoptosis and ROS production. Mechanistically, silibinin inhibited IR-induced DNA repair (ATM and Chk1/2) and EGFR signaling and attenuated the levels of anti-apoptotic proteins. Specifically, silibinin suppressed IR-induced nuclear translocation of EGFR and DNA-PK, an important mediator of DSB repair, leading to an increased number of γ-H2AX (ser139) foci suggesting lesser DNA repair. *In vivo*, silibinin strongly radiosensitized DU145 tumor xenograft inhibition (84%, P<0.01) with higher apoptotic response (10-fold, P<0.01) and reduced repair of DNA damage, and rescued the mice from IR-induced toxicity and hematopoietic injury. Overall, silibinin enhanced the radiotherapeutic response *via* suppressing IR-induced pro-survival signaling and DSB repair by inhibiting nuclear translocation of EGFR and DNA-PK. Since silibinin is already in phase II clinical trial for PCa patients, the present finding has translational relevance for radioresistant PCa.

Keywords

Radiosensitization; prostate cancer; EGFR; DNA repair; silibinin

*Corresponding author: Prof. Rana P. Singh, 104, Cancer Biology Laboratory, School of Life Sciences, Jawaharlal Nehru University, New Delhi, India-110067. Phone: +91-011-26704503, rana_singh@mail.jnu.ac.in & ranaps@hotmail.com.

Introduction

Radiotherapy is a frontline treatment option in prostate cancer (PCa), next only to radical prostectomy, with 25% of men aged 18-65 years and 42% of men aged 65-74 years undergoing radiation therapy (1). However, the positive facets of radiotherapy are moderated by its detrimental consequences on normal dividing cells and emergence of therapeutic resistance (2). Hence, development of novel radio-sensitizing agents with a capacity to improve therapeutic index mandates urgent attention.

The major mechanisms responsible for radiotherapeutic resistance are the activation of pro-survival and DNA repair pathways in response to IR (3,4). In general, IR-induced cell death is mediated by induction of double-stranded breaks (DSBs) in DNA, which leads to faulty cell division and death by mitotic catastrophe. However, in response to IR, the damaged cells also activate their DNA repair machinery including ATM and DNA-PK, which reduces the extent of radiation-induced damage and resultant death (5). IR also activates mitogenic signaling especially epidermal growth factor receptor (EGFR) (6), and IR-induced EGFR nuclear translocation which activates DNA repair pathways (7,8). Understandably, these mechanisms are unfavorable to the use of radiation in cancer treatment, and suggest that agents that could inhibit EGFR-mediated signaling and/or DNA repair following radiotherapy could be successful radiosensitizers.

Here, we have evaluated the radiosensitizing properties of a plant flavonoid silibinin in PCa, a malignancy with late stage radioresistance. Silibinin possesses strong anticancer activity against PCa in preclinical studies and is currently in Phase II clinical trial against PCa (9,10). Subsequently, we rationalized that silibinin could enhance radioresponse and may have additional translational potential. Indeed, our results suggested that silibinin preferentially sensitizes PCa cells to IR, reduces IR-induced systemic injury and tissue toxicity and in mice, and enhances radiotherapeutic index for PCa.

Materials and Methods

Cell lines and reagents

Human prostate carcinoma DU145, PC-3 and 22RV1 cells, mouse keratinocyte JB6 cells, human lung cancer A549 cells were from ATCC (Manassas, VA). DU145, 22RV1 and A549 cell lines were characterized by STR analysis in August 2013, and PC-3 in July 2015. JB6 cells were procured in January 2010. HEK-293 cells were purchased from National Centre for Cell Science, Pune, India in August 2010. Initially, cells were grown and frozen in liquid nitrogen. Cells grown from a vial were always monitored for their morphology and used for the experiments within five months. Other cell culture materials were from Himedia, India. Silibinin (MW = 482.4), RPMI media, Propidium iodide (PI), DCFH-DA, antibodies to Cdc25C, DNA-PK, β-Actin were obtained from Sigma Aldrich Chemical Co. (St. Louis, USA). Antibody for Cyclin B1, Cdc-2, PCNA and survivin, phospho-EGFR, ATM, phospho-Chk1, phospho-Chk2, Chk1, Chk2 and anti-rabbit peroxidase-conjugated secondary antibody were from Cell Signaling Technology (Danvers, MA). Tubulin and anti-

mouse peroxidase-conjugated secondary, goat anti-rabbit IgG was from Santa Cruz Biotech. (CA, USA). ECL detection system was from Millipore, India.

Cell culture and treatments

DU145, PC-3, A549 and 22RV1 cells were cultured in RPMI-1640 medium with 10% fetal bovine serum and Penicillin-Streptomycin at 37°C in 5% CO_2 incubator. HEK-293 cells were grown in DMEM with 10% FBS and JB6 cells in MEM medium with 5% FBS. Cells were treated with varying doses of radiation (2.5-10 Gy) and/or silibinin (25-100 μM), which was dissolved in dimethyl sulfoxide (DMSO). The treatment time varied from 3–72 h depending upon the experiment. An equal volume of DMSO (0.1% v/v) was present in each treatment.

Irradiation protocol

The cells were irradiated in ^{60}Co gamma chamber (Model 4000A, Bhabha Atomic Research Centre, Mumbai, India) at a dose rate of 4.6 Gy/min. For the animal experiment, mice were irradiated using RS 2000 Biological Irradiator (Rad Source Technologies) housed at Anschutz Medical campus, UC Denver, USA. The dose rate of the irradiator was 1.34 Gy/min. The silibinin and IR treatments were started when the tumor volume reached 200 mm^3. Silibinin was given as 200 mg/kg body weight/day in 0.5% CMC by oral gavage and immediately followed with the 1st dose of IR (2.5 Gy per fraction) on day 0. Silibinin treatment continued as 5 days/week and each IR fraction was separated by two days. The cumulative dose of 15 Gy (six doses each with 2.5 Gy) was given to the animals. After last dosing of silibinin and IR on day 15, the experiment was terminated on day 16.

Colony formation assay

Cells were seeded in 6-well plates (500 cells/plate). After 24 h of plating, cells were treated with respective doses of radiation and/or silibinin (co-treatment) and eventually cultured for 10 days; the colonies formed were fixed with ice-cold methanol: glacial acetic acid (3:1) for 10 min; and stained with 1% crystal violet. Plating efficiency was calculated by dividing the average number of colonies per well by the amount of cells plated. Survival fractions were calculated by normalization to the plating efficiency of appropriate control groups. Dose enhancement ratio (DER) was calculated as the ratio of radiation dose without silibinin to dose of radiation with silibinin required to achieve the same amount of cell kill. If DER is > 1, the agent is considered to be radiosensitizing, whereas a value <1, the agent is considered to be radioprotective.

Cell cycle analysis by flow cytometry

Cell cycle distribution was analyzed by flow cytometry using BD FACS Calibur by BD Biosciences and data was analyzed with ModFit LT software, as described in earlier studies (34).

Reverse Transcriptase PCR

Cells were seeded and grown in 100 mm culture plates to 70% confluency under regular growth conditions and were treated with silibinin (25 μM) and/or radiation (5 Gy) in 10%

serum supplemented RPMI-1640 medium. Total RNA was isolated using TRIZOL reagent and cDNA was synthesized as described earlier. This was followed by standard PCR reactions using gene specific forward and reverse primers (Supplementary Methods). PCR products were analyzed by running on 1% agarose gel stained with ethidium bromide and photographed under low intensity UV in GelDoc system (Applied Biosystems).

BrdU incorporation assay

Briefly, the cells were cultured in 96-well plates at a density of 5000 cells/100 μl/well in complete growth media. After 48 hours of respective treatments, the cells were labeled with BrdU using the Cell Proliferation ELISA, BrdU (colorimetric) Kit (Roche Applied Science, Indianapolis, IN) and the percent BrdU incorporation was measured in each treatment, as per the manufacturer's protocol.

Analysis of ROS levels

Cells were treated with DMSO or 25 μM silibinin and/or 5 Gy for 12, 24, 48 and 72 h. Cells were incubated with 20 μM DCF-DA during the last 30 min of treatment at 37°C. The probe was washed off with PBS and the cells were trypsinized, resuspended in PBS and analyzed for DCF positive cells by flow cytometry.

DNA fragmentation assay

At the end of the treatment time, cells were gently scraped and centrifuged at 1,000g for 5 min at 4°C following which the cells were lysed by adding 500 μl of the lysis buffer containing 1% NP-40, 20 mM EDTA, 5 mM Tris-HCl-pH, 8.0. The lysed sample was then centrifuge at 12,000g at 4°C for 20 min and the supernatant was collected and treated with RNase at 37°C for 1 h. The fragmented DNA was then extracted by phenol-chloroform method. Fragmented DNA was precipitated overnight at −20°C after adding 30 μL of 5 M NaCl to a final concentration of 300 mM and 2.5 volume of ice-cold 100% ethanol. The pellet obtained after centrifugation, was washed with 70% ethanol, air dried and resuspended in TE buffer and run on a 1.2% agarose gel containing 0.5 μg/ml ethidium bromide.

AO-EtBr apoptosis assay

After the completion of desired treatments, total cells were collected by centrifugation and added with 50 μl of staining solution containing the acridine orange (AO) and EtBr mix (100 μg/ml each) in PBS. Then cells were put on a slide and visualized under 100× field of a fluorescent microscope. A minimum of 250 cells were scored and percent apoptotic cells were determined. Early apoptotic cells showed green nuclei with condensed chromatin whereas late apoptotic cells showed orange nuclei with condensed chromatin.

Immunoblot analysis

PCa cells were grown in regular serum conditions to 70% confluency and treated with the desired doses of silibinin and/or radiation. At the end of the treatment time periods, whole cell lysates were prepared in non-denaturing lysis buffer as published recently (11). Cytoplasmic and nuclear extracts were prepared as described earlier (11). Protein

concentrations were determined by Bradford assay and 60-80 μg protein lysates were resolved on 8-16% SDS-PAGE. Proteins were blotted onto nitrocellulose membranes and probed with specific primary antibodies followed by detection with HRP-conjugated appropriate secondary antibodies employing ECL detection system.

Immunofluorescence staining assay

Cells were grown on coverslips in 24-well plate, washed with PBS, fixed in 4% formaldehyde for 15 min, and permeabilized with 0.3% TritonX-100 for 15 min. Cells were blocked with [10% (v/v) FBS, 0.3% (w/v) TritonX-100] for 1 h, incubated with a primary rabbit anti-pEGFR (1:200) or DNA-PKcs (1:250) overnight at 4°C and then incubated with the secondary antibody anti-rabbit IgG (1:500) for 1 h, and finally counterstained with 300 nM DAPI as published earlier (11). Cells were examined using a confocal microscope at our Central Instrument Facility in the school.

In vivo tumor xenograft study

Athymic (nu/nu) male nude mice (NCI Frederick, MD) approved by the Institutional Animal Care and Use Committee of the University of Colorado Denver were s.c. injected in the right flank with 6×10^6 DU145 cells mixed with matrigel. From the day following xenograft implantation, mice were monitored regularly for tumor growth and once the tumors reached approximately around 200 mm^3, the mice were randomly divided into four groups and respective treatments were given. For the radiation alone group, IR treatment (2.5 Gy / dose) was given at an interval of 2 days, till a cumulative dose of 15 Gy was achieved (day 15). Mice were anesthetized with ketamine/xylazine before radiation and positioned under a lead shield such that only the tumor-bearing flank was exposed. Silibinin (200 mg/kg) was given in 0.5% CMC (w/v) to animals as oral gavage just before the first dose of IR and continued for 5 days/week. Group I (vehicle control): 200 μl of 0.5% CMC (w/v) in saline; Group II: mice treated with IR alone, Group III: mice treated with IR and silibinin (SB); Group IV: mice treated with silibinin. Tumor sizes were measured twice weekly using digital caliper and tumor volume was calculated by the formula: 0.5236 L1 (L2)^2, where L1 is long diameter, and L2 is short diameter. Mice were sacrificed on day 16 (Figure 5A).

Immuno-histochemical analysis of tumors

After 24 h following the final irradiation and silibinin treatment, the mice were euthanized and tumors were dissected out, weighed, fixed in formalin and further processed and embedded in paraffin. Paraffin-embedded tissue sections were de-paraffinized and stained using specific primary antibody followed by 3, 3′-diaminobenzidine (DAB) staining, as previously described. Biotinylated secondary antibodies used were rabbit anti-mouse IgG (1:200; Dako) and goat anti-rabbit IgG (1:200; Santa Cruz). Apoptotic cells were identified by TUNEL staining using Dead End Colorimetric TUNEL System (Promega Corp., Madison, WI) as published (12). Percentage of Ki-67, TUNEL, pChk2, pH2A.X -positive cells were quantified by counting brown-stained cells within total number of cells at five arbitrarily selected fields from each tumor at 400× magnification.

Densitometric and statistical analyses

Bands on X-ray films were scanned and their mean density was analyzed by ImageJ (NIH, Bethesda, MD). Densitometry data, which is represented below the bands, are the 'fold change' as compared with respective DMSO control, after normalization with respective loading controls (β-actin). The data were statistically analyzed using the Jandel Scientific Sigma Stat 3.5 software. Student's t-test was employed for statistical significance (P<0.05). Paired student's *t*-test was used for tumor volumes.

Results

Silibinin preferentially radiosensitizes PCa cells

Effect of silibinin in sensitizing PCa cells to IR was assessed employing two radioresistant human PCa cell lines DU145 and PC-3 using clonogenic survival assays. PC-3 were more sensitive to IR treatment than DU145, showing 47% decrease in colony formation compared to 32% in DU145 at 5 Gy dose (Figure 1A & B). IR (2.5-10 Gy) inhibited colony formation by 17-68%, which increased to 29-92% (P<0.001) in combination with 25 μM silibinin in DU145 cells (Figure 1a). Similar results were observed for PC-3 cells (Figure 1C). The dose enhancement ratio (DER) at 50% inhibition in colony formation was 1.67 for DU145 and 1.4 for PC-3 cells. Silibinin also radiosensitized other type of cancer cells, e.g. human lung carcinoma A549 cells, with a dose enhancement ratio of 1.6 (Figure 1D). More importantly, in non-neoplastic human embryonic kidney cells (HEK-293), similar treatment with IR and/or silibinin did not radiosensitize the cells; in fact, it resulted in radioprotection with a DER of 0.83 at 50% inhibition (Figure 1E). In radioresponsive 22RV1 cells, combination treatment did not show any significant increase in radiosensitivity (Supplementary Figure 1).

Silibinin enhanced and prolonged IR-induced G2/M arrest of PCa cells

IR alone increased G2/M cell population from 20% in control to 37%, which was further increased to 59% (P<0.001) when combined with 25 μM silibinin at 24 h, and in the combination treatment, the effect was prolonged (P<0.01) even till 48 h (Figure 2A, left panel and Supplementary Figure 2). A similar trend in cell cycle effects was observed in PC-3 cells with combination treatment (Figure 2A, right panel). Concurrently, the expression levels of Cyclin B1 and Cdc2 decreased as early as 6 h following the combination treatment (Figure 2B). This effect was sustained till 48 h, where we also observed IR-induced increase in Cdc25C which was strongly decreased in the IR plus silibinin treatment, supporting prolonged G2/M block in the combination treatment (Figure 2B, right panel and Supplementary Figure 3A). In HEK-293 cells, combining SB with radiation did not show significant difference in gene expression of cell cycle regulators as compared with radiation treatment alone, which again suggests that silibinin shows a differential response. (Supplementary Figure 3A)

Silibinin strongly inhibited cancer cell proliferation following IR exposure and down-regulated IR-induced expression of pro-survival molecules

Following irradiation, a fraction of cells that are lethally damaged undergo apoptosis, but the remaining cells that are sub lethally irradiated try to evade apoptosis, by activating a pro-

survival response. After 48 h of treatment, BrdU incorporation decreased by 36% (P<0.001) in silibinin with IR as compared to IR alone (16%) in DU145 cells, whereas in PC-3 cells, combination treatment resulted in 39% (P<0.01) inhibition versus 30% in IR alone (Figure 2C). This inhibition was aided *via* decreased expression of both PCNA and survivin, which did not change with IR alone in DU145 cells (Figure 2D). In PC-3 cells, IR appeared to post-transcriptionally modify and increase protein levels of PCNA and survivin which were decreased by the combination treatment (Figure 2D and Supplementary Figure 3B).

Silibinin enhanced IR-induced ROS production and led to prolonged oxidative stress

Although, silibinin has antioxidant activity, it is now well documented that many polyphenols including silibinin also behave as pro-oxidants under certain conditions (13,14). We found that IR showed an established distribution pattern of ROS production during 12-72 h of treatments with a peak at 24 h, whereas silibinin showed peak of ROS production at ∼ 48 h, with 27% positive cells (Figure 2E, left panel). In the combination treatment, there was a dramatic increase in the ROS-positive cells with a peak at 24 h (61%, P<0.001) (Figure 2E and Supplementary Figure 4A & B). Combination of silibinin with IR also led to reduction in the mRNA expression of antioxidant enzymes including SOD1, SOD2, Catalase and GST, supporting the data showing enhanced oxidative stress in these cells (Supplementary Figure 4C).

Since instead of radiosensitization, we had observed radioprotection of HEK-293 cells by silibinin, we examined whether this differential effect could be facilitated *via* the modulation of redox status. Surprisingly, presence of silibinin with IR showed an inverse effect on HEK-293 cells to that of cancer cells. Silibinin treatment alone showed 7% ROS-positive cells, whereas in IR alone, there were 25% ROS-positive cells at 48 h (Figure 2E, right panel and Supplementary Figure 4D). However, combining silibinin with IR significantly reduced ROS-positive cells to 7.6% (P<0.001).

Silibinin enhanced IR-induced apoptosis

Since pro-survival molecules were suppressed and ROS level was enhanced in combination treatment, we assessed whether it led an increase in radiation-induced apoptosis. Compared to either silibinin or IR, an intense DNA laddering (>2 fold) in combination treatment was observed in both DU145 and PC-3 cells (Figure 3A). Acridine-orange- EtBr assay also showed an increase in apoptosis from 25-27% in IR alone to 44-46% (P<0.001) in combination after 48 h in both PCa cells (Figure 3B). Bcl-2 overexpression, a major player in the development of radioresistant phenotype (15), was up-regulated by IR in DU145 cells, whereas combining it with silibinin led to a profound decrease in Bcl-2 expression in DU145 cells with a moderate effect on PC-3 cells (Figure 3C).

Silibinin augmented the therapeutic efficacy of radiation by inhibiting DNA repair

One of the major mechanisms for acquired radioresistance in cancer cells is the DNA repair, DNA being the principle target of radiation-induced damage (16). Our results revealed that IR enhances ATM expression as early as 3 h but in combination treatment, especially at 6 h, it down-regulated the expression of ATM in DU145 cells (Figure 3D). Also, the phosphorylated level of EGFR (Y1068) was enhanced with IR, which was reduced by

silibinin treatment. Chk1 and Chk2, the downstream effectors of ATM involved in activation of DNA repair (17), were also induced by IR showing an increase in mRNA levels (Figure 3E) and enhanced phosphorylation of Chk1 (S345 and S269) and Chk2 (T68). These IR-induced levels were down-regulated in the combination treatment (Figure 3F).

Silibinin inhibited IR-induced nuclear translocation of EGFR

The role of nuclear EGFR in development of radioresistance by acting as a mediator for DNA repair is gaining grounds (6,8). Furthermore, IR-induced EGFR activation is a prominent contributor to radioresistance. Since, we observed inhibition of IR-activated EGFR, we further analyzed whether silibinin can alter IR-induced nuclear translocation of EGFR in PCa cells. IR exposure of DU145 cells resulted in nuclear translocation of EGFR (red) at 3 h that was almost completely inhibited by silibinin and EGFR localization was limited to the cytosol (Figure 4A). This was further confirmed by measuring EGFR protein levels in cytosolic and nuclear fractions (Figure 4B). We also checked the effect of these treatments on nuclear translocation of EGFR in non-neoplastic JB6 mouse keratinocyte cells (Supplementary Figure 5). Compared to PCa cells, we did not observe considerable reduction in the nuclear localization of EGFR in JB6 cells, suggesting that this effect of silibinin may be selective to neoplastic cells.

Silibinin inhibited IR-induced nuclear translocation of DNA-PK and prolonged the presence of pH2A.X foci

Confocal microscopy showed that after IR treatment, most of DNA-PK was localized into the nucleus. However, when cells were treated with silibinin and IR, like EGFR, DNA-PK too remained excluded out of the nucleus, thereby blocking it from carrying out its DNA repair function (Figure 4C). To further support that silibinin inhibits IR-induced DNA repair signaling, pH2A.X foci were assessed as indicator of DNA damage. We observed that IR exposure increased pH2A.X foci at 6 h, which was reduced by 12 h (59% decrease, P<0.001), whereas in presence of silibinin, it was increased by 38% (Figure 4D). Furthermore, by 12 h in the presence of silibinin, the number of pH2A.X foci was more than 2.5 fold (P<0.001) from that of IR alone (Figure 4D). This persistence of pH2A.X foci levels in combination as compared with IR alone suggests that silibinin-mediated radiosensitization involves an inhibition of repair of IR-induced DNA damage.

Silibinin enhanced radiation-induced tumor-growth inhibition and protected the normal tissue from radiation injury

After establishing the radiosensitizing properties of silibinin *in vitro*, we substantiated these findings in DU145 xenograft model. Once the tumors reached ∼200 mm³, mice were treated with IR and/or silibinin, as detailed in the Materials and Methods (Figure 5A). Silibinin and IR inhibited tumor growth (volume) by 56% (P<0.01) and 61% (P<0.01) from control, respectively; however their combination led to 84% (P<0.001) growth inhibition when compared to control (Figure 5B). Similarly, tumor weight was decreased by 46% (P<0.01), 43% (P<0.01), and 82% (P<0.001) in silibinin, IR and IR with silibinin treated groups from control, respectively (Figure 5C). The tumor volume and weight were decreased by 61% (P<0.01) and 69% (P<0.01) in combination when compared with IR alone, respectively.

IR treatment alone led 13% and 30% decrease in body weight and diet consumption, respectively, at the end of treatment; however, silibinin treatment reversed these losses by 8% and 19% (P<0.01 for both), respectively (Figure 5D & E). IR leverages heavy toxicity to the hematopoietic system (17). We observed that total WBC, neutrophil, monocyte and platelet counts were reduced by 33-50% by IR; however, treatment with silibinin completely blocked (P<0.01-0.001) these adverse effects of IR on hematopoietic system (Figure 5F-H, Supplementary Figure 6B-E). We also observed a lesser damage to genitourinary tract (GUT) (Supplementary Figure 6A). These results indicate that the combination treatment was not toxic to normal tissues and in fact, silibinin showed radioprotective response in normal tissues.

Silibinin-mediated radiosensitization of prostate tumor involved inhibition of DNA repair and enhanced apoptosis

The immunohistochemical analysis of tumor samples showed that IR and/or silibinin reduced the immunostaining for Ki67 (Figure 6A). IR or silibinin alone decreased Ki67-positive cells by 25% and 21%, respectively; however, their combination resulted in 54% (P<0.001) decrease versus control, and 33% (P<0.01) versus IR alone treatment (Figure 6B), which supported the corresponding decrease in tumor burden. For the translational relevance of the *in vitro* observations of DNA repair signaling, tumors were analyzed for the pChk2 (Figure 6A & C), which was increased by ~7 fold (P<0.001) by IR treatment and that was reduced by the silibinin treatment to ~2 fold (P<0.001) when compared with control (Figure 6C). Next, the DNA DSBs were analyzed by immunostaining of pH2A.X (S139) (Figure 6A & B), which was increased to 4% as compared to 1% in control, whereas in combination with silibinin, as anticipated, it increased to 13% (P<0.001), suggesting that the mechanism of silibinin-mediated radiosensitization involved reduced DSB repair signaling (Figure 6D). By TUNEL staining of tumor tissue (Figure 6A), no significant apoptosis induction was observed with radiation or silibinin alone while their combination increased apoptotic cells by 10 fold (P<0.001) from control and 5 fold (P<0.001) from IR treatment (Figure 6E).

Discussion

Radiotherapy is one of the principal and affordable treatment choices for locally or regionally advanced PCa (18). However, development of radioresistance in these cells delimits its effectiveness in patients. With an aim to strengthen therapeutic outcomes, radiotherapy is often used in combination with drugs which are either cytotoxic or can radiosensitize or both (19,20). These agents help in achieving the required remission at a much lower dose of radiation thereby reducing the damage to normal tissues, which is a very germane issue in cancer treatment. However, currently, there is barely any radiosensitizer that has been successful in clinics.

In the current study, we demonstrated the radiosensitizing effects of silibinin in PCa cells. Silibinin enhanced the efficacy of radiation therapy in PCa *via* (a) enhancing and prolonging the G2/M cell cycle arrest induced by IR, (b) augmenting ROS levels and sustaining high level of oxidative stress, (c) inhibiting IR-induced pro-survival signaling and anti-apoptotic pathways, (d) inhibiting IR-induced DNA repair signaling in PCa cells and tumors. These

mechanisms eventually contributed to decreased cell growth, clonogenicity and increased cell death; subsequently improving radiotherapeutic response. Additionally, silibinin also helped in countering IR-induced toxicity in normal tissues.

One of the mechanisms for radiosensitizing effect of a drug could be its ability to affect cell cycle progression especially by blocking it in G2/M phase of the cell cycle (21). Our study found that silibinin could enhance IR-induced G2/M arrest and also prolongs the duration of the arrest. This is of high significance in fractionated radiotherapy, G2/M phase being the most radiosensitive phase in the cell cycle, arresting a maximal population of cells in this phase would subsequently sensitize them to next cycle of radiation and enhance cell killing (22).

Other than cell cycle perturbations, radiation-induced damage is essentially orchestrated *via* the production of ROS, which targets macromolecules, causing severe damage leading to cell death (23). Radiation-induced ROS levels peak within minutes of exposure and after the peak, it maintains a medium level of ROS lasting for days after irradiation (24). Unlike in normal cells, this moderate level of ROS is well tolerated by cancer cells, as these cells manipulate their redox system and generally have high levels of antioxidant enzymes to counter these conditions (25,26). It has also been shown that in cancer stem cells, persistent low levels of ROS could eventually help in development of radioresistance (27). We demonstrated that addition of silibinin along with IR, can dramatically increase the level of ROS which, when retained for a longer duration, overpowers the robust antioxidant defense in cancer cells and drives the cell to death. Thus, silibinin enhances the ionizing radiation-induced oxidative stress to a level where it doesn't contribute to development of resistance, instead maintains it high and persistent enough to induce cell death. Another significant finding was that silibinin showed this pro-oxidant behavior exclusively in cancer cells, but not in normal cells. This biased behavior in modulating the redox status of cancer cells is a valuable asset for a radiosensitizer. This finding could also explain the disparity in response observed in clonogenic assay with HEK-293 cells when compared with other cancer cells.

Studies done in the past looking at the mechanisms of radioresistance in PCa have pointed out that the up-regulation of pro-survival signaling and the tipping of the balance towards anti-apoptosis, compromises with the therapeutic efficacy of IR. The overexpression of Bcl-2 enhances radiation resistance in PCa and other cancer cells (28,29) and the suppression of which could overcome resistance (15). We demonstrate that silibinin could down-regulate IR-induced survival signaling. Silibinin down-regulated IR-induced Bcl-2 and survivin expression in DU145 and PC-3 cells, thereby maneuvering the cells towards apoptosis. Most cancer cells boast of a robust DNA repair system, which also contributes to acquiring a radioresistant phenotype. Thus, DNA repair proteins are now regarded as key targets for radiosensitization (16,30). Our study found that silibinin could down-regulate the repair process by inhibiting the expression of ATM as well as other downstream effectors including Chk1 and Chk2.

One of the major players, which is involved in both DNA repair and up-regulation of pro survival signaling is EGFR (7,8). Most of the earlier studies linking EGFR and radioresistance focused on the receptor signaling induced by EGFR after ligand independent

activation in response to IR (31). But recent literature suggests that in response to IR, EGFR could contribute directly to development of radioresistance by its role in the nuclear compartment where it regulates DNA repair along with DNA-PK, which is a key regulator of NHEJ (7,8,32,33). We found that silibinin treatment blocked nuclear translocation of EGFR. Silibinin also modulated the distribution of DNA-PK, restraining it from entering the nucleus to carry out its function, in concurrence with EGFR. The exclusion of EGFR and DNA-PK from the nucleus prevented the repair of DNA lesions, as shown by significantly enhanced number of γ-H2A.X foci. This is the first report of a phytochemical modulating DNA repair by blocking the nuclear translocation of EGFR.

Many radiosensitizers though seem effective *in vitro*, but do not work under *in vivo* conditions and also have problems associated with toxicity. IR and silibinin combination strongly decreased tumor burden and also reduced Ki67-positive cells in these tumors. We also observed intense staining for γ-H2A.X and inhibition in Chk2 phosphorylation, suggesting inhibition of DNA repair signaling induced by IR. From our previous PCa xenograft study (34), we know that the selected oral dose of silibinin used for the combination with IR is non-toxic. We observed significant reduction in the body weight and diet consumption in the IR alone group; however, the combination showed substantial improvement in these parameters. We also found that systemic toxicity of IR, mainly on the hematopoietic system was greatly reduced by silibinin treatment.

In conclusion, we, for the first time, report that silibinin functions as a potent radiosensitizer in human PCa cells, and more importantly it offers substantial protection to the normal tissues from unwarranted IR toxicity. Silibinin targets multiple pathways including DNA repair signaling involving nuclear translocation of EGFR, which are implicated in development of radioresistance (Figure 6F). Earlier studies done with silibinin showed that a concentration of up to 100 μM could be achieved in blood plasma in mouse (35) as well as in humans (36), which signifies that the dose used in study (25 μM) could be realized in patients undergoing radiotherapy for PCa, and thus underlines the translational significance of this study.

Supplementary Material

Refer to Web version on PubMed Central for supplementary material.

Acknowledgments

References

1. Siegel R, DeSantis C, Virgo K, Stein K, Mariotto A, Smith T, et al. Cancer treatment and survivorship statistics, 2012. CA Cancer J Clin. 2012; 62:220–41. [PubMed: 22700443]
2. Begg AC, Stewart FA, Vens C. Strategies to improve radiotherapy with targeted drugs. Nat Rev Cancer. 2011; 11:239–53. [PubMed: 21430696]

3. Burdak-rothkamm S, Prise KM. New molecular targets in radiotherapy : DNA damage signalling and repair in targeted and non-targeted cells. Eur J Pharmacol. 2009; 625:151–5. [PubMed: 19835868]

4. Powell SN, Abraham EH. The biology of radioresistance : similarities, differences and interactions with drug resistance. Cytotechnology. 1993; 12:325–45. [PubMed: 7764455]

5. Tichý A, Vávrová J, Pejchal J, Rezácová M. Ataxia-telangiectasia mutated kinase (ATM) as a central regulator of radiation-induced DNA damage response. Acta Medica. 2010; 53:13–7. [PubMed: 20608227]

6. Bai J, Guo XG, Bai XP. Epidermal growth factor receptor-related DNA repair and radiation-resistance regulatory mechanisms: a mini-review. Asian Pac J Cancer Prev. 2012; 13:4879–81. [PubMed: 23244074]

7. Brand TM, Iida M, Luthar N, Starr MM, Huppert EJ, Wheeler DL. Nuclear EGFR as a molecular target in cancer. Radiother Oncol. 2013; 108:370–7. [PubMed: 23830194]

8. Chen DJ, Nirodi CS. The epidermal growth factor receptor: a role in repair of radiation-induced DNA damage. Clin Cancer Res. 2007; 13:6555–60. [PubMed: 18006754]

9. Deep G, Agarwal R. Antimetastatic efficacy of silibinin: molecular mechanisms and therapeutic potential against cancer. Cancer Metastasis Rev. 2010; 29:447–63. [PubMed: 20714788]

10. Ting H, Deep G, Agarwal R. Molecular mechanisms of silibinin-mediated cancer chemoprevention with major emphasis on prostate cancer. AAPS J. 2013; 15:707–16. [PubMed: 23588585]

11. Nambiar DK, Deep G, Singh RP, Agarwal C, Agarwal R. Silibinin inhibits aberrant lipid metabolism, proliferation and emergence of androgen-independence in prostate cancer cells via primarily targeting the sterol response element binding protein 1. Oncotarget. 2014; 5:10017–33. [PubMed: 25294820]

12. Kaur M, Velmurugan B, Tyagi A, Deep G, Katiyar S, Agarwal C, et al. Silibinin suppresses growth and induces apoptotic death of human colorectal carcinoma LoVo cells in culture and tumor xenograft. Mol Cancer Ther. 2009; 8:2366–74. [PubMed: 19638451]

13. Bhaumik S, Anjum R, Rangaraj N, Pardhasaradhi BV, Khar A. Curcumin mediated apoptosis in AK-5 tumor cells involves the production of reactive oxygen intermediates. FEBS Lett. 1999; 456:311–4. [PubMed: 10456330]

14. Galati G, Sabzevari O, Wilson JX, O'Brien PJ. Prooxidant activity and cellular effects of the phenoxyl radicals of dietary flavonoids and other polyphenolics. Toxicology. 2002; 177:91–104. [PubMed: 12126798]

15. An J, Chervin AS, Nie A, Ducoff HS, Huang Z. Overcoming the radioresistance of prostate cancer cells with a novel Bcl-2 inhibitor. Oncogene. 2007; 26:652–61. [PubMed: 16909121]

16. Zhu Y, Hu J, Hu Y, Liu W. Targeting DNA repair pathways : A novel approach to reduce cancer therapeutic resistance. Cancer Treat Rev. 2009; 35:590–6. [PubMed: 19635647]

17. Smith J, Tho LM, Xu N, Gillespie DA. The ATM-Chk2 and ATR-Chk1 pathways in DNA damage signaling and cancer. Adv Cancer Res. 2010; 108:73–112. [PubMed: 21034966]

18. Szostak MJ, Kyprianou N. Radiation-induced apoptosis: predictive and therapeutic significance in radiotherapy of prostate cancer (review). Oncol Rep. 2014; 7:699–706. [PubMed: 10854529]

19. Belka C, Jendrossek V, Pruschy M, Vink S, Verheij M, Budach W. Apoptosis-modulating agents in combination with radiotherapy-current status and outlook. Int J Radiat Oncol Biol Phys. 2004; 58:542–54. [PubMed: 14751526]

20. Nambiar D, Rajamani P, Singh RP. Effects of phytochemicals on ionization radiation-mediated carcinogenesis and cancer therapy. Mutat Res Rev. 2011; 728:139–57.

21. Leonard CE, Chan DC, Chou TC, Kumar R, Bunn PA. Paclitaxel enhances in vitro radiosensitivity of squamous carcinoma cell lines of the head and neck. Cancer Res. 1996; 56:5198–204. [PubMed: 8912857]

22. Pawlik TM, Keyomarsi K. Role of cell cycle in mediating sensitivity to radiotherapy. Int J Radiat Oncol Biol Phys. 2004; 59:928–42. [PubMed: 15234026]

23. Valerie K, Yacoub A, Hagan MP, Curiel DT, Fisher PB, Grant S, et al. Radiation-induced cell signaling: inside-out and outside-in. Mol Cancer Ther. 2007; 6:789–801. [PubMed: 17363476]

24. Werner E, Kandimalla R, Wang H, Doetsch PW. A role for reactive oxygen species in the resolution of persistent genomic instability after exposure to radiation. J Radiat Res. 2014; 55(Suppl 1):i14.

25. Toyokuni S, Okamoto K, Yodoi J, Hiai H. Persistent oxidative stress in cancer. FEBS Lett. 1995; 358:1–3. [PubMed: 7821417]

26. Szatrowski TP, Nathan CF. Production of large amounts of hydrogen peroxide by human tumor cells. Cancer Res. 1991; 51:794–8. [PubMed: 1846317]

27. Diehn M, Cho RW, Lobo NA, Kalisky T, Dorie MJ, Kulp AN, et al. Association of reactive oxygen species levels and radioresistance in cancer stem cells. Nature. 2009; 458:780–3. [PubMed: 19194462]

28. Condon LT, Ashman JNE, Ell SR, Stafford ND, Greenman J, Cawkwell L. Overexpression of Bcl-2 in squamous cell carcinoma of the larynx: a marker of radioresistance. Int J Cancer. 2002; 100:472–5. [PubMed: 12115532]

29. Rosser CJ, Reyes AO, Vakar-Lopez F, Levy LB, Kuban DA, Hoover DC, et al. Bcl-2 is significantly overexpressed in localized radio-recurrent prostate carcinoma, compared with localized radio-naive prostate carcinoma. Int J Radiat Oncol Biol Phys. 2003; 56:1–6. [PubMed: 12694817]

30. Helleday T, Petermann E, Lundin C, Hodgson B, Sharma RA. DNA repair pathways as targets for cancer therapy. Nat Rev Cancer. 2008; 8:193–204. [PubMed: 18256616]

31. Schmidt-Ullrich RK, Mikkelsen RB, Dent P, Todd DG, Valerie K, Kavanagh BD, et al. Radiation-induced proliferation of the human A431 squamous carcinoma cells is dependent on EGFR tyrosine phosphorylation. Oncogene. 1997; 15:1191–7. [PubMed: 9294612]

32. Liccardi G, Hartley JA, Hochhauser D. EGFR nuclear translocation modulates DNA repair following cisplatin and ionizing radiation treatment. Cancer Res. 2011; 71:1103–14. [PubMed: 21266349]

33. Raju U, Riesterer O, Wang ZQ, Molkentine DP, Molkentine JM, Johnson FM, et al. Dasatinib, a multi-kinase inhibitor increased radiation sensitivity by interfering with nuclear localization of epidermal growth factor receptor and by blocking DNA repair pathways. Radiother Oncol. 2012; 105:241–9. [PubMed: 23010482]

34. Singh RP, Raina K, Deep G, Chan D, Agarwal R. Silibinin suppresses growth of human prostate carcinoma PC-3 orthotopic xenograft via activation of extracellular signal-regulated kinase 1/2 and inhibition of signal transducers and activators of transcription signaling. Clin Cancer Res. 2009; 15:613–21. [PubMed: 19147767]

35. Agarwal C, Singh RP, Dhanalakshmi S, Tyagi AK, Tecklenburg M, Sclafani RA, et al. Silibinin upregulates the expression of cyclin-dependent kinase inhibitors and causes cell cycle arrest and apoptosis in human colon carcinoma HT-29 cells. Oncogene. 2003; 22:8271–82. [PubMed: 14614451]

36. Flaig TW, Gustafson DL, Su LJ, Zirrolli JA, Crighton F, Harrison GS, et al. A phase I and pharmacokinetic study of silybin-phytosome in prostate cancer patients. Invest New Drugs. 2007; 25:139–46. [PubMed: 17077998]
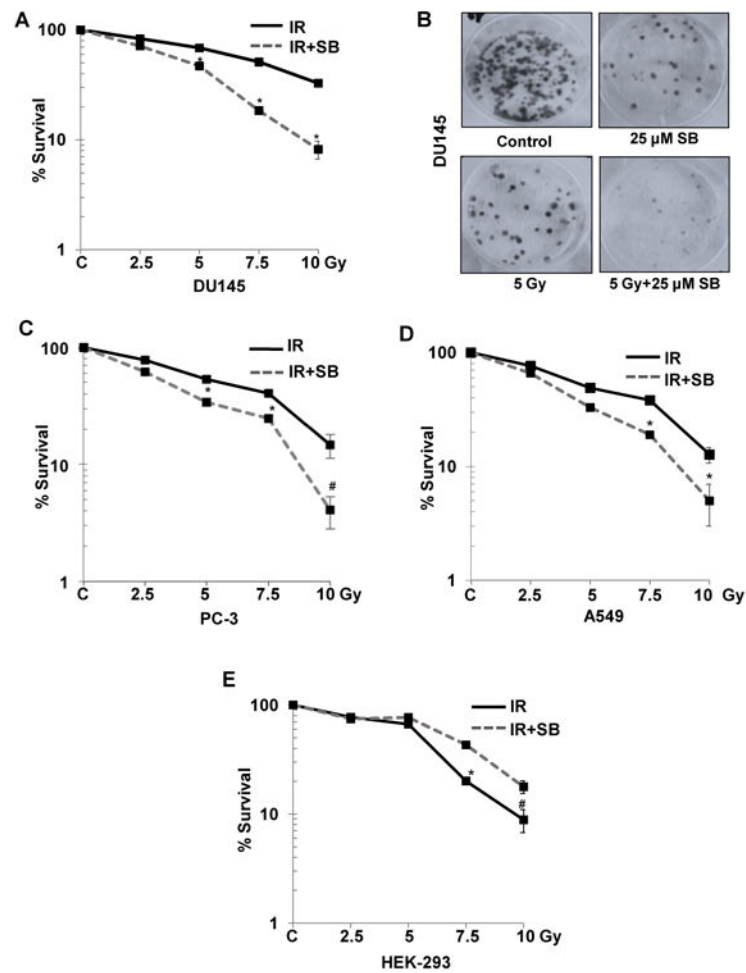
Figure 1. Silibinin selectively radiosensitizes PCa cells
Cells were plated at 600 cells/ well in a 6-well plate and after 24 h treated with the indicated dose of ionizing radiation (IR) and/or 25 μM of silibinin (SB). Cells were then maintained for another 10 days. The colonies were fixed and stained. Number of colonies containing >50 cells were counted and percent colony formation was determined for each cell line with respect to the non-treated controls. Survival curves for (**A**) advanced human prostate carcinoma DU145 with (**B**) Representative picture for stained colonies of DU145 cells, (**C**) PC-3 cells, (**D**) A549 cells, and (**E**) transformed non-neoplastic human embryonic kidney, HEK-293 cells are shown. P<0.01 (#), P<0.001(*) compared with respective control
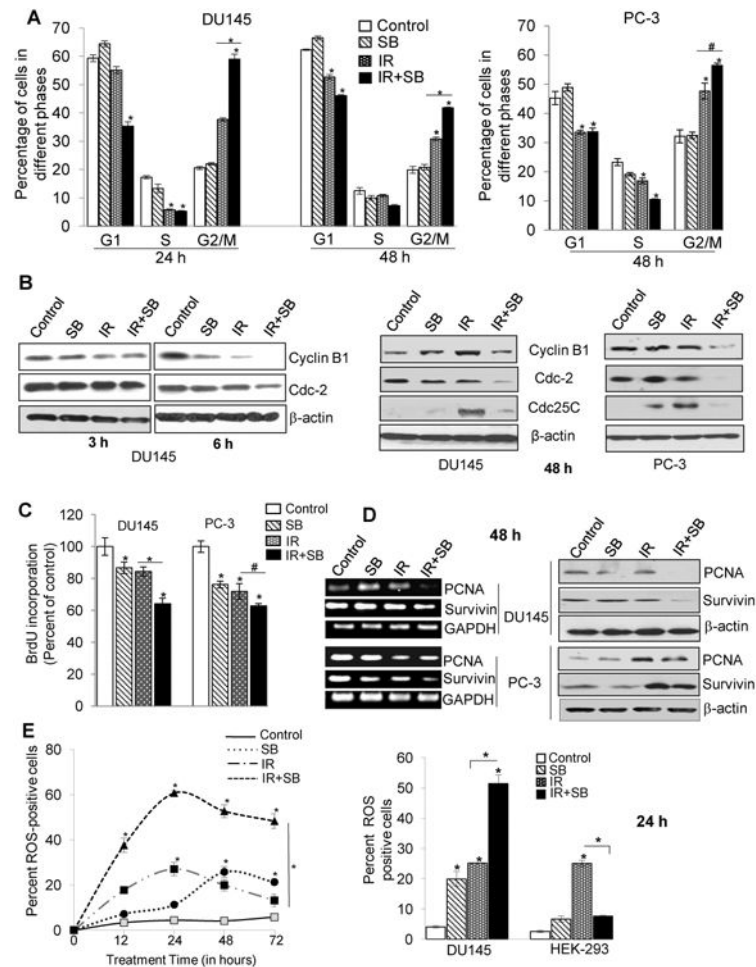
Figure 2. Silibinin potentiates IR-induced G2/M arrest, inhibition in cell proliferation and augments the oxidative stress selectively in PCa cells

DU145 and PC-3 cells were exposed to ionizing radiation (IR) with or without silibinin (SB). After treatment time points, cells were processed for cell cycle analysis using saponin-PI staining (**A**) Quantitative data showing cell cycle distribution in DU145 (left panel) and PC-3 cells (right panel) after treatment with IR (5 Gy) and/or SB (25 μM). (**B**) Western blots for G2/M cell cycle related proteins at 3 h, 6 h and 48 h. Cell proliferation rate in cells was assessed by BrdU incorporation assay. (**C**) Percent BrdU incorporation was calculated with respect to control after 48 h treatment in both DU145 and PC-3 cells. (**D**) RT-PCR and immunoblotting analysis of PCNA and survivin proteins after 48 h treatment. (**E**) For oxidative stress analysis, Cells were analyzed for DCF fluorescence by flow cytometry, after treatment with IR (5 Gy) and/or SB (25 μM). Percent positive cells were those with a fluorescent intensity $>10^2$ on the histogram. Graph showing change in the DCF positive cells in different groups after 12-72 h of treatment of DU145 cells. Bar diagram showing DCF-positive cells for DU145 and HEK-293 cells after 24 h of treatment.
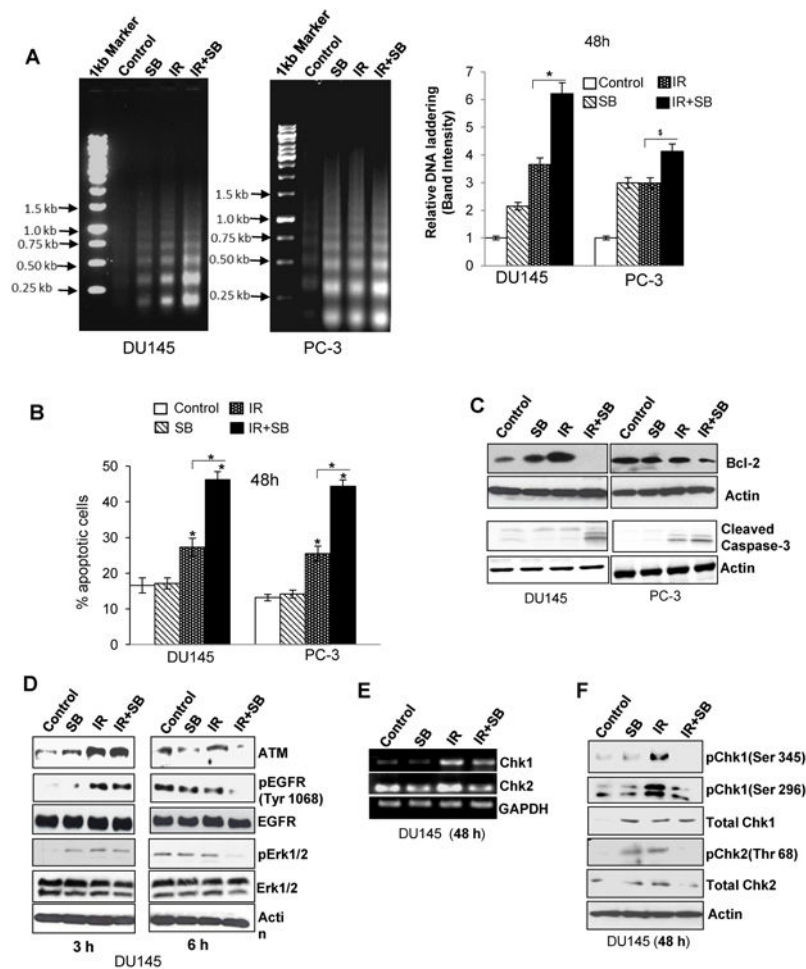
Figure 3. Silibinin potentiates radiation-induced apoptosis and attenuates DNA repair activation signaling in PCa cells

(**A**) Representative pictures (left panel) and quantitative data (right panel) showing DNA laddering in DU145 and PC-3 cells treated with IR (5 Gy) and/or silibinin (25 μM) for 48 h. (**B**) Graphical data depicting percent cells positive for apoptosis after Acridine orange –EtBr staining. (**C**) Western blot analysis of Bcl-2 and cleaved caspase-3 in DU145 and PC-3 cells after 48 h of treatment. (**D**) Immunoblotting for damage signaling molecules activated in response to IR (5 Gy) and/or SB (25 μM). (**E**) RT-PCR for cell cycle check-point regulators Chk1 and Chk2; and (**F**) phospho/total Chk1 (threonine 345 and serine 296) and Chk2 levels (threonine 68) in DU145 cells.
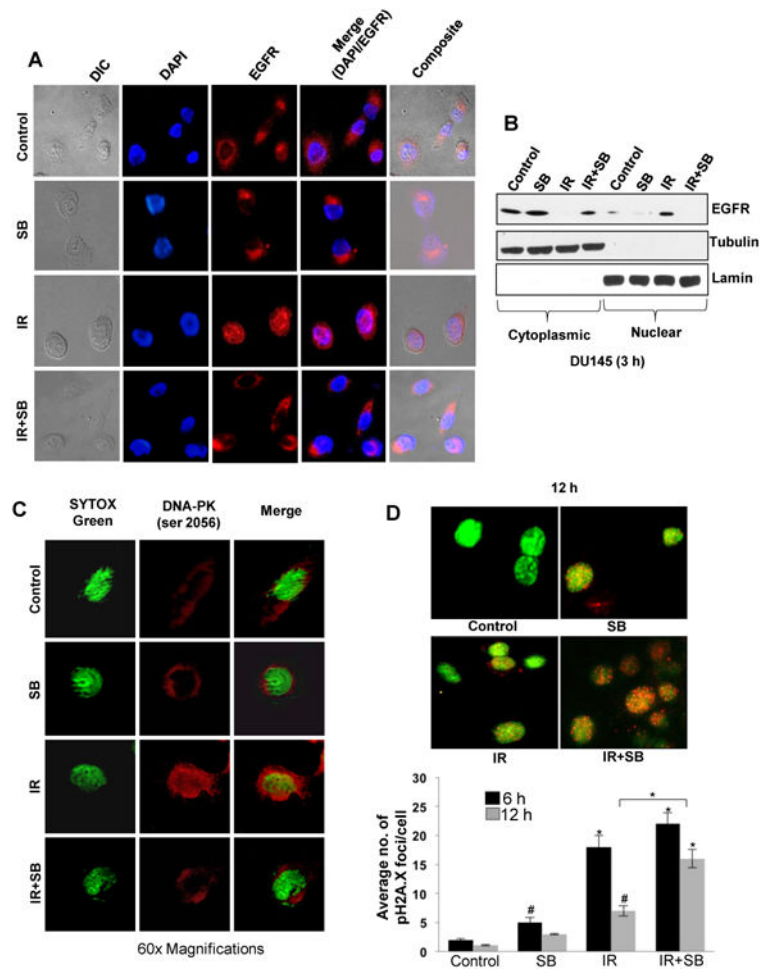
Figure 4. Silibinin inhibits nuclear translocation of EGFR and DNA-PK in cancer cells and reduces repair of pH2A.X (Ser 139) foci in PCa cells

(**A**) Confocal microscopy showing distribution of EGFR (red) in DU145 cells in response to IR (5 Gy) and/or SB (25 μM). (**B**) Immunoblotting for EGFR in cytoplasmic and nuclear fractions after 3 h of treatments; tubulin and lamin were used as loading control for cytoplasmic and nuclear compartments, respectively. (**C**) Confocal microscopy showing distribution of DNA-PK (red), nucleus (Sytox-green) in DU145 cells in response to IR (5 Gy) and/or SB (25 μM) at 3 h; and (**D**) Representative images of pH2A.X foci (red) in the nucleus at 12 h and quantitation of number of pH2A.X foci after 6 and 12 h of treatments in DU145 cells.
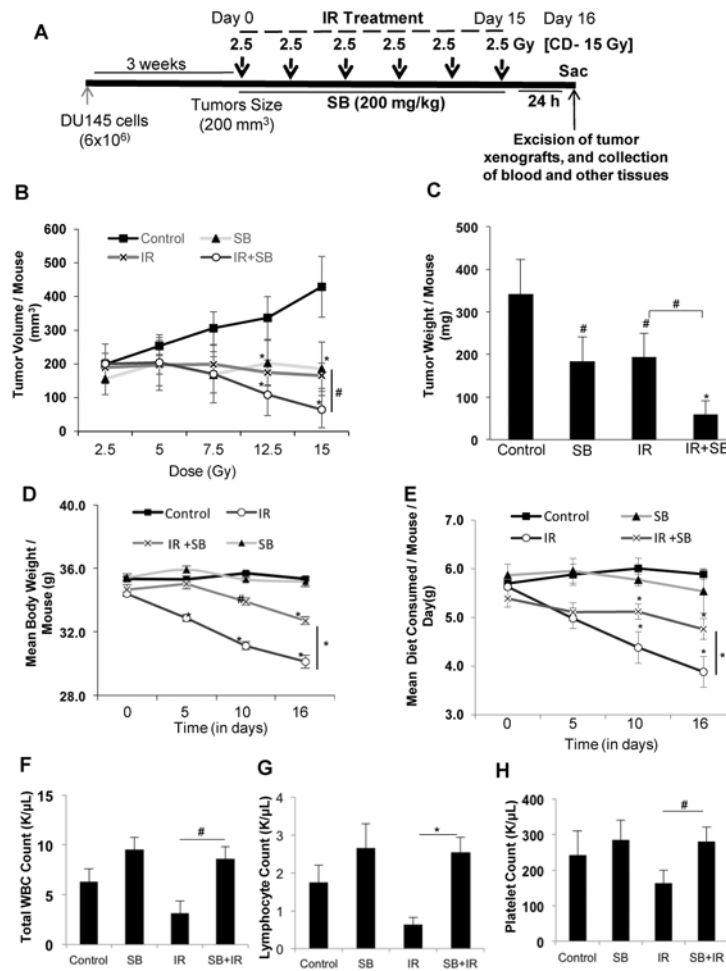
Figure 5. Silibinin treatment enhances radiation-induced tumor growth inhibition of human PCa DU145 xenograft in athymic nude mice

(**A**) Diagrammatic representation of the time line followed for the tumor study. Mice were subcutaneously injected with DU145 cells (6×10^6) mixed with Matrigel (1:1) and monitored for tumor growth till the tumor size reached $\sim$200 mm^3. Then mice were treated with IR (2.5 Gy) with a gap of two days between two IR fractions, with or without SB (200 mg/kg), which was given 5 days/week. Control and IR alone group of mice were gavaged with 0.5% CMC in saline. The treatment was continued till the cumulative irradiation dose reached 15 Gy. Twenty four hours after the final fraction of IR (day 16), the tumors were excised and processed further for immune-histochemical staining. (**B**) Tumor volume/mouse as a function of cumulative radiation dose, (**C**) tumor weight/mouse at the end of study, (**D**) mean body weight/mouse, and (**E**) average diet consumption/mouse/day were analyzed as detailed in Materials and Methods. Data shown in mean ± SE from 8 mice in each group. Effect of IR and/or silibinin was also checked on the hematopoietic system at the end of the experiment (**F**) Mean WBC count/ mouse, (**G**) Mean lymphocyte count/mouse and (**H**) represents mean platelet count/mouse. P<0.05 ($); P<0.01 (#), P<0.001(*) compared with respective control.
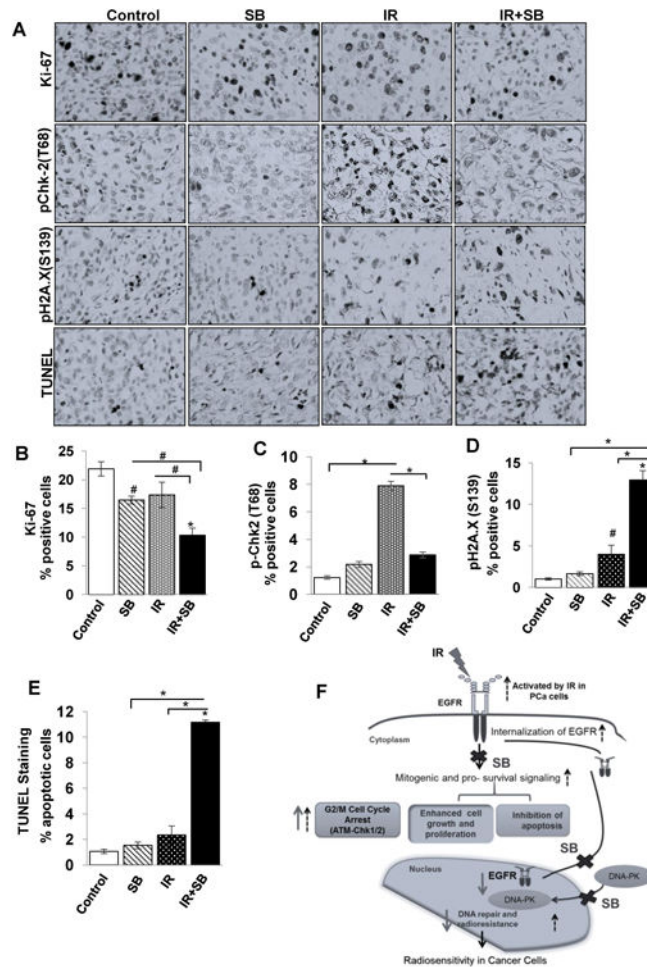
Figure 6. Combination of silibinin with IR leads to reduced expression of cell proliferation and DNA repair markers and enhances apoptosis in DU145 xenograft

Tumor xenograft tissue samples were immunohistochemically analyzed for Ki67, pChk-2 (T68), pH2A.X and TUNEL-positive cells as detailed in Materials and Methods. (**A**) The representative pictograph (400× magnifications) for positive brown-stained cells (dark color) for each of the marker are shown from control, IR, SB and IR+SB groups. Quantitative data for (**B**) Ki67, (**C**) pChk-2(T68), (**D**) pH2A.X(S139) and (**E**) apoptotic cells from 5–6 mice in each group. P<0.01 (#), P<0.001(*) compared with respective control. (**F**) A model summarizing the radiosensitizing action of silibinin in PCa cells. Black dotted arrows represent pathways activated by IR in PCa cells, bold arrows represent the action of silibinin (SB) and crosses represent IR-activated responses blocked by silibinin.